Heterocyclic Letters
Vol. 13| No.1|115-127|November -January|2023
ISSN : (print) 2231–3087 / (online) 2230-9632
CODEN: HLEEAI
http://heteroletters.org

SYNTHESIS, CHARACTERIZATION AND IN-SILICO STUDIES OF 1, 4-DISUBSTITUTED 1, 2, 3-TRIAZOLE 4-FORMYL BENZOATE

Nayana R[a], Krishnaswamy G*[a], Lubna Kouser[a], Nayana J[a], Manjushree G R[a], Kavya B[a], Lokesh P[a], Shivaraj G[a,b], Sreenivasa S[b,c] and Suresh D[a]

[a]Department of Studies and Research in Organic Chemistry, Tumkur University, Tumakuru-572 103, Karnataka, India
[b]Department of Studies and Research in Chemistry, University College of Science, Tumkur University, Tumakuru-572 103, Karnataka, India
[c]Deputy Adviser, National Assessment and Accreditation Council, Bengaluru-560 072, Karnataka, India
**Corresponding author (E-Mail: drkrishna23org@gmail.com)*

ABSTRACT:
In continuation to our interest on 1, 2, 3-triazoles, in the present study we report the synthesis, characterization and *in-silico* studies of novel 4-formyl benzoate 1, 4-disubstituted 1, 2, 3-triazoles. The newly synthesised compounds structures were confirmed based on the spectroscopic data (^{1}H & ^{13}C NMR) and were in good agreement with the assigned structures. From PASS prediction result revealed that compounds may act as better antimycobacterial agents. Further, ADME assessments were carried out to check pharmaceutical associated properties of the compounds. All the compounds possess “drug like” properties with low toxicity. Finally molecular docking studies were carried out on anti-tubercular target protein PDB ID: 4FDO to predict mechanism of action and validate PASS prediction.

KEYWORDS: Formyl benzoate, Triazole, PASS, ADME and molecular docking studies.

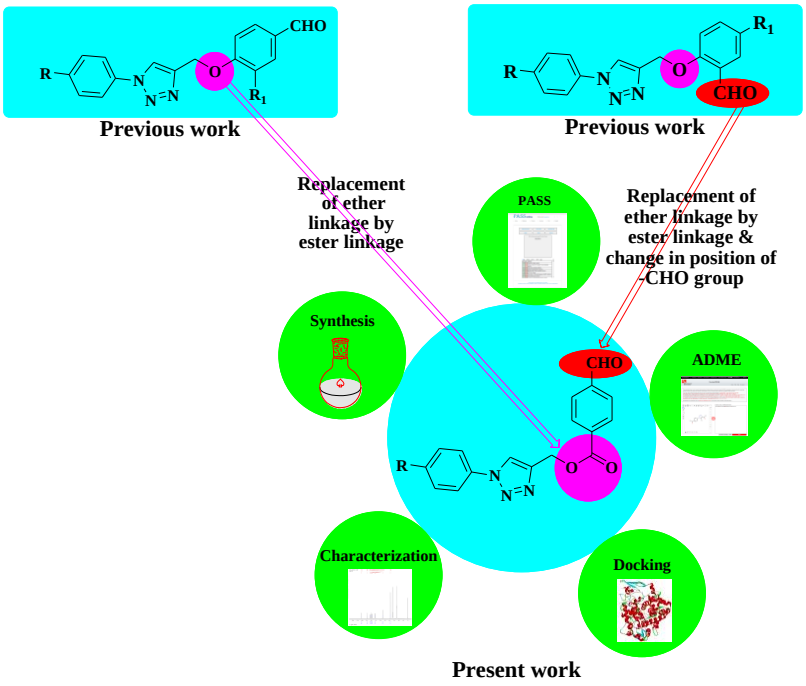

INTRODUCTION:

Tuberculosis is the among leading infectious disease cause for the death because of failures in the treatment due to development of multidrug resistance tuberculosis (MDR-TB) and extensively drug resistant tuberculosis (XDR-TB) which pose new challenges for the prevention, treatment and control [i]. Hence, there is an emergency need to develop a new inhibitors since *Mycobacterum tuberculosis* (MTB) developed resistance to the first line and second line drugs currently used for the treatment [ii]. Among the heterocyclic compounds, 1,2,3-triazoles gained much interest in medicinal chemistry since they interact easily with biomolecular targets via hydrogen bond, dipole-dipole and π stacking interactions with high stability resisting robust oxidative and reductive conditions [iii]. Moreover, 1,2,3-triazole derivatives have been reported to show promising anti-tubercular activity profile (figure-1) [iv-vii] along with wide range of biological applications [viii].

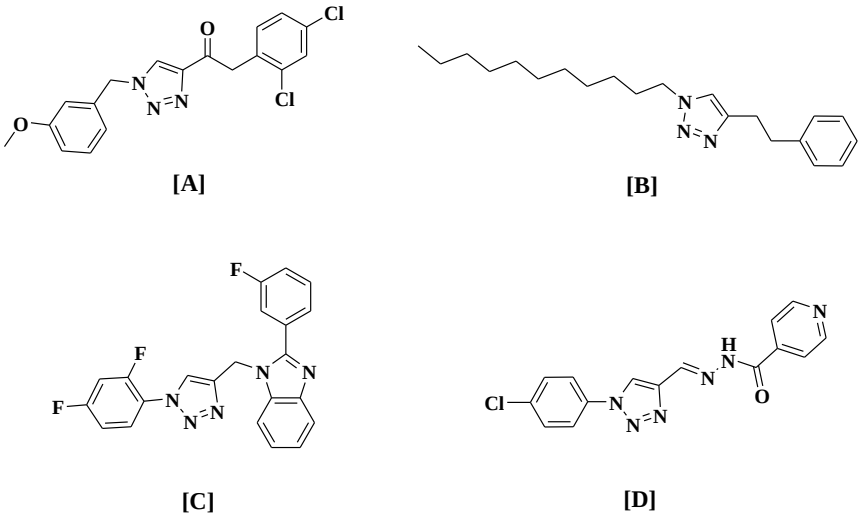

Figure-1: Anti-tubercular agents with 1,2,3-traizole moiety

On the other hand, there are reports that formyl (CHO) group in the organic compounds act as high level disinfectants in health care environments [ix,x] and used in the preparation of herbicides as well as plant growth regulators [xi,xii]. Based on the above highlights on the importance and in continuation of our earlier work [xiii] on 1,2,3-triazole derivatives, a small library of 1,2,3-triazole compounds with formyl group with ester linkage have been efficiently prepared via Click approach is reported. In addition to this, synthesised compounds have been evaluated for their possible biological profile via PASS, pharmaceutical associated properties via ADME and mechanism of action via molecular docking studies.

Scheme-1: Synthetic route of 1, 4-Disubstituted 1, 2, 3-triazole 4-Formyl benzoate

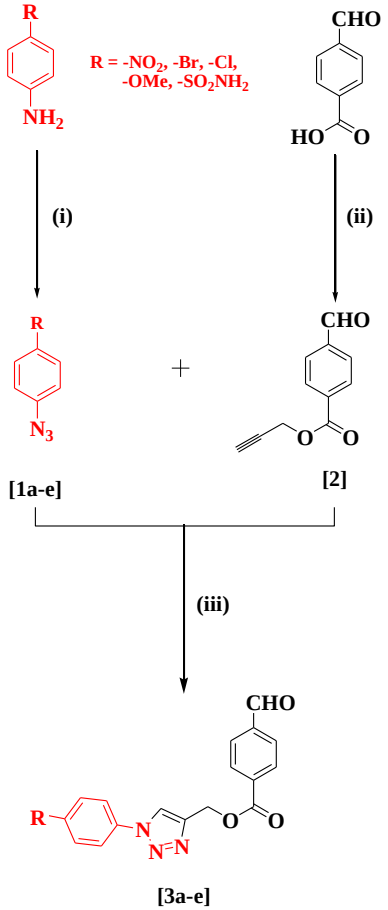

[3a-e]

Reagents and Condition: (i) $NaNO_2$, HCl, NaN_3, 0°C-rt, 1 hr.; **(ii)** Propargyl bromide, K_2CO_3, DMF, rt, 24 hr; **(iii)** $CuSO_4.5H_2O$, Sodium Ascorbate, THF:H_2O, rt.

EXPERIMENTAL SECTION:

Materials and Instrumentation

The organic solvents and chemicals were purchased from SD Fine, Spectrochem, Sigma Aldrich and standard commercial sources are used without further purification. Room temperature reactions mentioned ranges between 15-35°C. For low temperatures reactions an ice-bath with sodium chloride (0°C) was used. Magnetically stirred oil bath (or) heated on a hotplate were used for heating reactions. Progress of the reactions was monitored by TLC using Merck silica gel 60 F_{254} precoated on aluminium backed plates. Spots on the TLC plates were visualized with ultraviolet light or iodine vapors or by staining with 2% aqueous potassium permanganate solution wherever necessary. The ^1H and ^{13}CNMR spectra were recorded on

Agilent (400 MHz, ^{1}H NMR) and (100 MHz, ^{13}C NMR) spectrometers using deuteriated solvents ($CDCl_3$ or DMSO-d_6) and Tetramethylsilane (TMS) as an internal standard.

GENERAL PROCEDURE

Synthesis of Prop-2-ynyl 4-formylbenzoate [2]

4-Formyl benzoic acid (1.0 mmol) and anhyd K_2CO_3 (2.0 mmol) were added to a round bottom flask of 100 mL containing 10 mL of DMF and the resulting mixture was stirred at lab temperature for 24 hrs. The reaction was followed by thin layer chromatography. After completion of reaction, dilute the reaction mixture with 10 mL of water and resulted in formation of precipitate. The precipitated product was collected through filtration, washed with water and dried. Further obtained product was triturated with ethyl acetate and hexane.

Synthesis of (1-(4-nitrophenyl)-1H-1, 2, 3-triazol-4-yl) methyl 4-formylbenzoate [3a]

To a solution of 1-azido-nitrobenzene **[1a]** (1.0 mmol) in a 1:1 mixture of THF and water (10 mL) taken in 100 mL round bottom flask, $CuSO_4.5H_2O$ (10 mol %), Sodium Ascorbate (20 mol %) and prop-2-ynyl 4-formylbenzoate **[2]** (1.0 mmol) were added with stirring. The resulting mixture was stirred at lab temperature for 8–12 hrs. The consumption of the starting materials was monitored using TLC. The reaction mixture was diluted with ethyl acetate and washed with water followed by a saturated solution of sodium chloride and dried over anhydrous sodium sulphate. The organic layer was evaporated under vacuum to residue further triturating with chloroform and hexane resulted in the desired solid product of (1-(4-nitrophenyl)-1H-1, 2, 3-triazol-4-yl) methyl 4-formylbenzoate **[3a].** Following above procedure remaining 1, 2, 3-triazole derivatives **[3b-e]** were synthesized.

PASS Analysis:

PASS (prediction of activity spectra for substances) available online: http://www.way2drug.com/passonline/ is the computer program used for computational screening of possible biological activities of drug like candidates. PASS can be used to estimate the biological activity profile for virtual molecule prior to their chemical synthesis and biological testing.

ADME evaluation

For a molecule to be called as a successful drug candidate is decided by its good potential and satisfactory ADME profile. Nowadays, it is recommended to screen ADME (Absorption, Distribution, Metabolism, and Excretion) properties as early as possible in the drug discovery process so as to reduce failures. The online search engines SwissADME was used to evaluate the ADME properties [xiv].

Molecular docking studies

In-silico molecular docking is a computational technique plays important role in the rational design of drugs and widely used to predict the binding orientation of small molecule drug candidates to protein targets in order to predict the affinity and activity of the small molecule.

Molecular targets of anti-tubercular agents

The 1, 2, 3-triazole derivatives have been reported to inhibit DprE1 (decaprenylphosphoryl-β-Dribose-2'-epimerase) enzyme which involved in the biosynthesis of decaprenylphosphoryl-D-arabinose (DPA), an essential component of the mycobacterial cell wall of MTB [xv,xvi]. Hence, DprE1 enzyme (PDB ID: 4FDO) was chosen for docking studies in order to investigate the binding interactions of the synthesized compounds.

Protein preparation:

Based on the PASS prediction, PDB structure i.e., PDB: 4FDO was downloaded from the free protein database https://www.rcsb.org/structure/4FDO. The protein structure was prepared

using discovery studio visualizer to remove all non-receptor atom including water, ion and miscellaneous compounds and the cleaned protein structure then was saved as pdb file.

Ligand preparation:

The structure of native ligand from the target macromolecules was prepared by discovery studio visualizer to separate from the protein, water, miscellaneous substances and saved as pdb file. Non-polar hydrogen atoms, gasteiger charges and the rotatable bonds were set by using AutoDock 4.2 tools and saved as pdbqt file. The ligands **[3a-e], [ISO]** and **[PYR]** were drawn on Chem Draw Ultra 8.0, assigned with proper 2D orientation and were converted to energy minimized 3D structures using discovery studio visualizer and saved as pdb files. Non-polar hydrogen atoms, gasteiger charges and the rotatable bonds were set by using AutoDock 4.2 tools and saved as pdbqt file.

Docking method validation

To ensure that the docking studies were valid and represented the reasonable potential binding model, the docking methods and parameters used were validated by redocking experiment. Each copy of native ligand was docked into the native protein to determine the ability of Autodock program to reproduce the orientation and position of the ligand observed in the crystal structure. The valid criteria used is the all atom root mean square deviation (RMSD) between the docked position and the crystallographically observed binding position of the ligand, and success is typically regarded as being less than 2 Å.

Docking studies

Docking studies were carried out using the above mentioned prepared target macromolecule and ligands **[3a-e], [ISO]** and **[PYR]** by employing Autodock Vina program [xvii]. All the docking runs were performed in Intel Centrino Core2 Duo CPU @ 2.20GHz of IBM system origin, with 4 GB DDR2 RAM run under Microsoft Windows operating system.

RESULTS AND DISCUSSION

Chemistry

Diazotization reaction of substituted aromatic primary amines with $NaNO_2$/HCl at lower temperature (0-5ºC) followed by nucleophilic substitution with sodium azide afforded corresponding substituted azido benzene derivatives **[1a-e].** Further, substituted azido benzene derivatives **[1a-e]** underwent Cu (I)-catalyzed Huisgen 1, 3-dipolar cycloaddition reaction at lab temperature with prop-2-ynyl 4-formylbenzoate **[2]** to get corresponding 1, 4-substituted-1, 2, 3-triazole derivatives **[3a-e]** respectively in good to excellent yield as depicted in **Scheme-1**. The newly synthesised compounds structures were confirmed based on the spectroscopic data (^{1}H & ^{13}C NMR) and were in good agreement with the assigned structures. In the proton NMR spectra, absence of triplet signal at 2.56-2.54 ppm due to alkyne proton and presence of singlets in the range of δ 8.88 to 9.18 and 5.53 to 5.56 ppm indicates the protons of triazole ring and methylene groups respectively confirms the formation of triazole derivatives. Further the presence of characteristic chemical shift for the triazole ring carbons in the range of δ 142.96-143.96 and δ 120.40-122.35 ppm in the ^{13}C NMR spectra confirms the formation of 1, 4-Disubstituted 1, 2, 3-Triazole 4-Formyl benzoate regioisomer [xviii,xix]. The detailed spectral data for the intermediate **[2]** and 1, 4-substituted-1, 2, 3-triazole derivatives **[3a-e]** were given the following section.

Prop-2-ynyl 4-formylbenzoate [2]

^{1}H NMR ($CDCl_3$, δ ppm): 10.11 (s, 1H, CHO), 8.52-8.23 (m, 2H, Ar-H), 7.98-7.95 (m, 2H, Ar-H), 4.97-4.96 (d, 2H, CH_2), 2.56-2.54 (t, 1H, CH); **^{13}C NMR (DMSO-d_6, δ ppm):** 192.86 (CHO), 164.26 (COO), 139.30, 133.58, 129.92, 129.68, 78.23, 78.07, 52.99 (CH_2).

(1-(4-nitrophenyl)-1H-1, 2, 3-triazol-4-yl) methyl 4-formylbenzoate [3a]

^{1}H NMR (DMSO-d_6, δ ppm): 10.09 (s, 1H, CHO), 9.18 (s, 1H, Triazole-H), 8.45-8.43 (d, 2H, Ar-H), 8.25-8.22 (d, 2H, Ar-H), 8.19-8.17 (d, 2H, Ar-H), 8.04-8.02 (d, 2H, Ar-H), 5.55 (s, 2H, CH_2); **^{13}C NMR (DMSO-d_6, δ ppm):** 193.39 (CHO), 165.16 (COO), 143.96, 141.19, 139.77, 130.49, 130.11, 126.01, 124.06, 121.26, 58.65 (CH_2).

(1-(4-bromophenyl)-1H-1, 2, 3-triazol-4-yl) methyl 4-formylbenzoate [3b]

^{1}H NMR (DMSO-d_6, δ ppm): 10.11 (s, 1H, CHO), 9.02 (s, 1H, Triazole-H), 8.20-8.18 (d, 2H, Ar-H), 8.06-8.04 (d, 2H, Ar-H), 7.92-7.90 (m, 2H, Ar-H), 7.83-7.81 (m, 2H, Ar-H), 5.54 (s, 2H, CH_2); **^{13}C NMR (DMSO-d_6, δ ppm):** 192.86 (CHO), 164.66 (COO), 142.98, 139.23, 135.66, 133.90, 132.73, 129.97, 129.59, 123.12, 122.05, 121.46, 58.24 (CH_2).

(1-(4-chlorophenyl)-1H-1, 2, 3-triazol-4-yl) methyl 4-formylbenzoate [3c]

^{1}H NMR (DMSO-d_6, δ ppm): 10.12 (s, 1H, CHO), 9.02 (s, 1H, Triazole-H), 8.20-8.19 (d, 2H, Ar-H), 8.06-8.04 (d, 2H, Ar-H), 7.99-7.97 (d, 2H, Ar-H), 7.70-7.68 (d, 2H, Ar-H), 5.55 (s, 2H, CH_2); **^{13}C NMR (DMSO-d_6, δ ppm):** 192.86 (CHO), 164.66 (COO), 142.96, 139.23, 135.25, 13.90, 133.06, 129.97, 129.81, 129.95, 123.11, 121.83, 58.24 (CH_2).

(1-(4-methoxyphenyl)-1H-1, 2, 3-triazol-4-yl) methyl 4-formylbenzoate [3d]

^{1}H NMR (DMSO-d_6, δ ppm): 10.11 (s, 1H, CHO), 8.88 (s, 1H, Triazole-H), 8.20-8.18 (d, 2H, Ar-H), 8.06-8.04 (t, 2H, Ar-H), 7.83-7.82 (q, 2H, Ar-H), 7.15-7.13 (q, 2H, Ar-H), 5.53 (s, 2H, CH_2), 3.83 (s, 3H, OCH_3); **^{13}C NMR (DMSO-d_6, δ ppm):** 193.45 (CHO), 165.23 (COO), 159.84, 143.05, 139.74, 134.47, 130.51, 130.40, 130.15, 123.61, 122.35, 115.36, 58.87 (CH_2), 56.05 (CH_3).

(1-(4-sulfonamidophenyl)-1H-1, 2, 3-triazol-4-yl) methyl 4-formylbenzoate [3e]

^{1}H NMR (DMSO-d_6, δ ppm): 10.12 (s, 1H, CHO), 9.10 (s, 1H, Triazole-H), 8.21-8.15 (q, 4H, Ar-H), 8.07-8.01 (q, 4H, Ar-H), 7.54 (s, 2H, SO_2NH_2), 5.56 (s, 2H, CH_2); **^{13}C NMR (DMSO-d_6, δ ppm):** 192.91 (CHO), 164.96 (COO), 143.95, 143.20, 139.29, 138.90, 133.90, 130.01, 129.63, 127.47, 123.36, 120.40, 58.23 (CH_2).

PASS Analysis:

The PASS results showed that the synthesised compounds **[3a-e]** display wide range of biological activities and in this study we focused our interest on antimycobacterial activity (Pa > 0.7) and compared predicted results for the synthesised compounds with standard anti-tubercular drugs isoniazid **[ISO]** and pyrazinamide **[PYR]** as tabulated in **table-1**.

Table-1: Predicted biological activity of compounds using PASS

Code	Biological Activity							
	Antimycobacterial		Antibacterial		Anti-inflammatory		Antifungal	
	Pa	Pi	Pa	Pi	Pa	Pi	Pa	Pi
3a	0.808	0.004	0.446	0.022	0.412	0.090	0.300	0.081
3b	0.788	0.004	0.398	0.097	0.405	0.029	0.295	0.083
3c	0.718	0.005	0.373	0.037	0.506	0.055	0.299	0.081
3d	0.729	0.005	0.394	0.032	0.500	0.057	0.268	0.096
3e	0.671	0.006	0.382	0.035	0.504	0.056	-	-
ISO	0.798	0.004	0.371	0.038	-	-	0.201	0.136
PYR	0.533	0.015	0.224	0.098	-	-	0.176	0.154

Pa-Probable to be active; **Pi**-Probable to be inactive

ADME evaluation:

Oral bioavailability prediction based on bioavailability radar

Bioavailability Radar considers six physicochemical properties: lipophilicity, size, polarity, solubility, flexibility and insaturation to depict oral bioavailability of molecule.

✓ **Orally bioavailable:** If the calculated physicochemical properties fall in the pink area of the radar plot.

✓ **Not orally bioavailable:** Any calculated property lie outside the pink area.

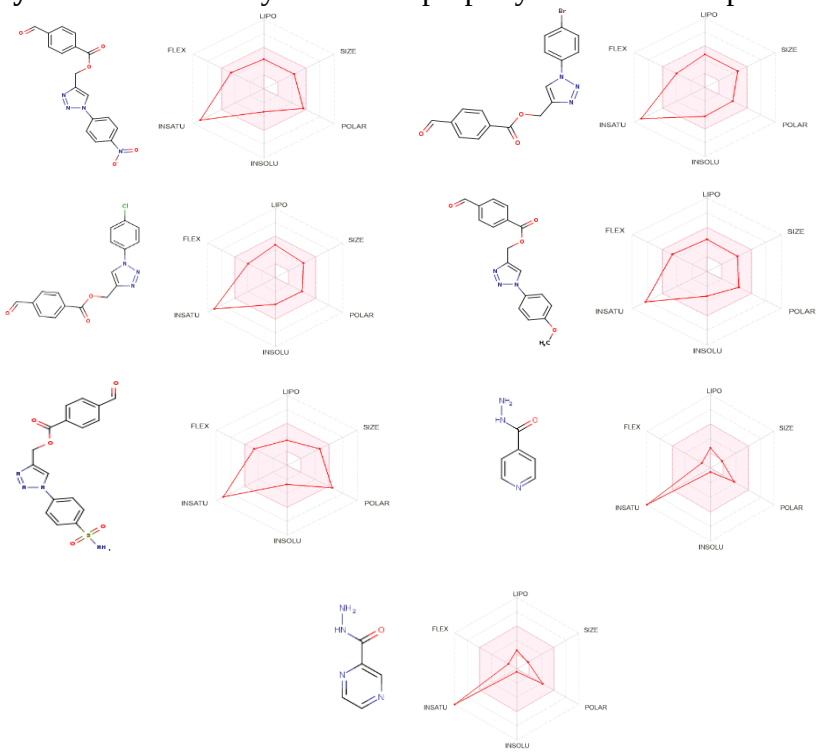

Figure-2: Two-dimensional structure and Bioavailability radar of [3a-e]

For the synthesized compounds **[3a-e]** bioavailability radar is as depicted in **figure-2** and all the compounds including standard drugs are not orally bioavailable because sp3 hybridization less than 0.25 as tabulated in **table-2**.

Table-2: Optimal range of properties for oral bioavailability

Standard range	**Code**						
	3a	**3b**	**3c**	**3d**	**3e**	**ISO**	**PYR**
LIPO (Lipophilicity): -0.7 < **XLOGP3** < +5.0	2.03	2.88	2.82	2.16	0.76	-0.70	-0.95
SIZE: 150g/mol < **MV** < 500g/mol	352.30	386.20	341.75	337.33	386.38	137.14	138.13
POLAR (Polarity): 20 Å^2 < **TPSA** < 130 Å^2	119.90	74.08	74.08	83.31	142.62	68.01	80.90
INSOLU (Insolubility): -6 < **Log S (ESOL)** < 0	-3.32	-4.18	-3.86	-3.33	-2.72	-0.56	-0.41
INSATU (Insaturation): 0.25 < **Fraction Csp3** < 1	0.06	0.06	0.06	0.11	0.06	0.00	0.00
FLEX (Flexibility): 0 < **Num. rotatable bonds** < 9	7	6	6	7	7	2	2

Physicochemical properties

Simple molecular and physicochemical descriptors like molecular weight (MW), molecular refractivity (MR), count of specific atom types and polar surface area (PSA) are compiled in this section and these parameters useful with regards to biological barrier crossing such as absorption and brain access. The predicted physicochemical properties of compounds are tabulated in **table-3**.

Table-3: Physicochemical properties of compounds

Code	Molecular Weight	Number of heavy atoms	Molar Refractivity	TPSA Å^2
3a	352.30	26	91.34	119.90
3b	386.20	24	90.21	74.08
3c	341.75	24	87.52	74.08
3d	337.33	25	89.01	83.31
3e	386.38	27	93.51	142.62
ISO	137.14	10	35.13	68.01
PYR	138.13	10	32.93	80.90

Lipophilicity

The partition coefficient between *n*-octanol and water (log $P_{o/w}$) is the classical descriptor for *Lipophilicity*. SwissADME gives five predictive models i.e. XLOGP3, WLOGP, MLOGP, SILICOS-IT and iLOGP. The Log Po/w value (WLOGP) is used to decide the non-aqueous solubility, a molecule is more soluble if the log Po/w value is more negative. Results showed that compounds **[3a-e]** were not soluble in non-aqueous medium (**table-4**).

Water solubility

Having a soluble molecule greatly facilitates many drug development activities, primarily the ease of handling and formulation. To estimate this qualitative estimation of solubility log S scale was used: if log S < −10 - poorly soluble, < −6 - moderately soluble, < −4 - soluble, < −2 - very soluble, and < 0 highly soluble. Low water solubility leads to bad absorption and therefore, the general aim is to avoid poorly soluble compounds. Based from these predictive models, standard drugs **ISO** & **PYR** were very soluble, synthesized compounds **[3a]** & **[3c-e]** were predicted to be soluble and compound **[3b]** was moderately soluble as shown in **table-4**.

Table-4: Predicted Lipophilicity and water solubility of compounds

Code	Log Po/w (WLOGP)	Log S (ESOL)	Solubility Class
3a	2.19	-3.32	Soluble
3b	3.05	-4.18	Moderately soluble
3c	2.94	-3.86	Soluble
3d	2.29	-3.33	Soluble
3e	2.01	-2.72	Soluble
ISO	-0.31	-0.56	Very soluble
PYR	-0.92	-0.41	Very soluble

Pharmacokinetics

The predictions for passive human gastrointestinal absorption (HIA) and blood-brain barrier (BBB) permeation is based on the BOILED-Egg model. The white region is for high probability of passive absorption by the gastrointestinal tract, and the yellow region (yolk) is

for high probability of brain penetration. Yolk and white areas are not mutually exclusive. In addition the points are coloured in blue if predicted as actively effluxed by P-gp (PGP+) and in red if predicted as non-substrate of P-gp (PGP−). Compounds **[3b]** & **[3c]** were predicted as brain penetrant (in the yolk) and not subjected to active efflux (red dot), while compounds **[3a], [3d], ISO** & **PYR** were predicted to be well absorbed in gastrointestine (in the white) but not has access to brain and PGP− (red dot). Compound **[3e]** predicted not GI absorbed and not BBB permeant with PGP− (red dot) and TPSA of 142.62 $Å^2$ as shown in **figure-3**.

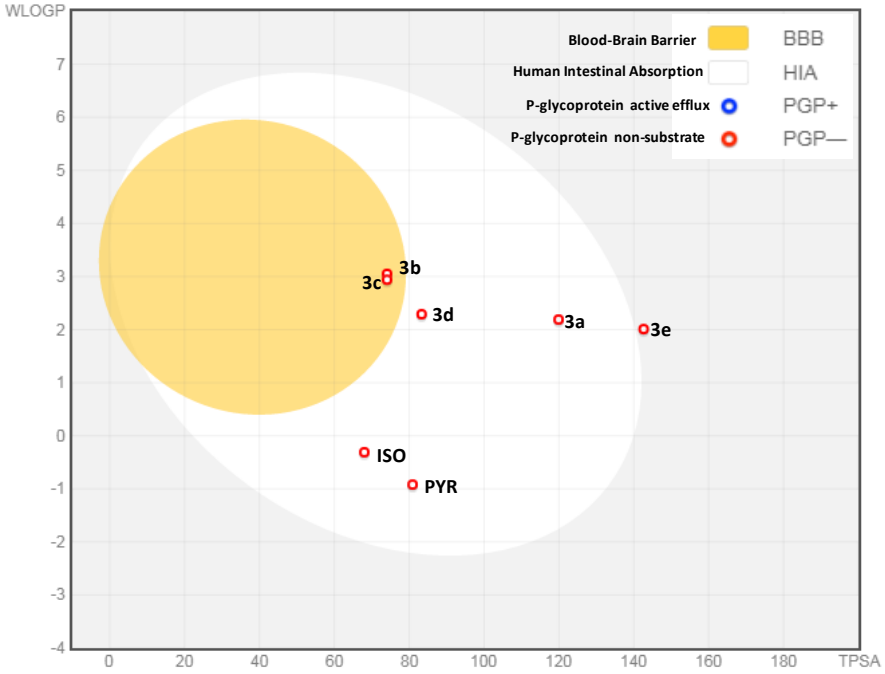

Figure-3: BOILED Egg image of compounds [3a-e] and standard drugs

A molecule is said to be less skin permeant if the value of log Kp is more negative. From the predicted results, compounds **[3a-e]**, **ISO** and **PYR** were found to be the least skin per- meant (**table-5**).

Table-5: Predicted distribution parameters in ADME of compounds

Code	GI absorption	BBB permeant	Log Kp (cm/s)
3a	High	No	-7.01
3b	High	Yes	-6.61
3c	High	Yes	-6.38
3d	High	No	-6.82
3e	Low	No	-8.12
ISO	High	No	-7.63
PYR	High	No	-7.82

The knowledge about compounds being substrate or non-substrate of the permeability glycoprotein and also knowledge about interaction of molecules with cytochromes P450 (CYP) superfamily of isoenzymes is a key in drug elimination through metabolic biotransformation. One can estimate therapeutic molecules whether they act as substrate or non substrate of five major isoforms (CYP1A2, CYP2C19, CYP2C9, CYP2D6, CYP3A4). Inhibition of these isoenzymes is certainly one major cause of pharmacokinetics-related drug-drug interactions

leading to toxic or other unwanted adverse effects due to the lower clearance and accumulation of the drug or its metabolites (**table-6**).

Table-6: Predicted metabolism parameters in ADME of compounds

Code	P-gp	CYP1A2 inhibitor	CYP2C19 inhibitor	CYP2C9 inhibitor	CYP2D6 inhibitor	CYP3A4 inhibitor
3a	No	Yes	Yes	Yes	No	No
3b	No	Yes	Yes	Yes	No	No
3c	No	Yes	Yes	Yes	No	No
3d	No	Yes	Yes	Yes	No	No
3e	No	No	No	No	No	No
ISO	No	No	No	No	No	No
PYR	No	No	No	No	No	No

Drug-likeness based on RO5, Ghose and Veber rules

This section gives access different rule-based filters, with diverse ranges of properties inside of which the molecule is defined as drug-like. The Lipinski (Pfizer) filter is the pioneer rule-of-five, Ghose (Amgen) and Veber (GSK) methods were adapted. Both compounds obey all the rules and may be considered as drug like as tabulated in **table-7**.

Table-7: Drug likeness of compounds

Code	Drug likeness								
	Lipinski				Ghose			Veber	
	MW ≤ 500	MlogP ≤ 4.15	N or O ≤ 10	NH or OH ≤ 5	160 ≤ MW ≤ 480	40 ≤ MR ≤ 130	20 ≤ atoms ≤ 70	Rotatable bonds ≤ 10	TPSA ≤ 140
3a	352.30	1.14	7	0	352.30	91.34	26	7	119.90
3b	386.20	2.65	5	0	386.20	90.21	24	6	74.08
3c	341.75	2.53	5	0	341.75	87.52	24	6	74.08
3d	337.33	1.73	6	0	337.33	89.01	25	7	83.31
3e	386.38	0.60	8	1	386.38	93.51	27	7	142.62
ISO	137.14	-0.47	3	2	137.14	35.13	10	2	68.01
PYR	138.13	-1.68	4	2	138.13	32.93	10	2	80.90

Molecular docking studies

First, the validation method was conducted to ensure the capability of docking machine. Figure represents the validation result of docking protocol. Redocking ligand showed similar conformation with the native ligands and the RMSD values were ≤ 2.0 Å as depicted in **figure-4**.

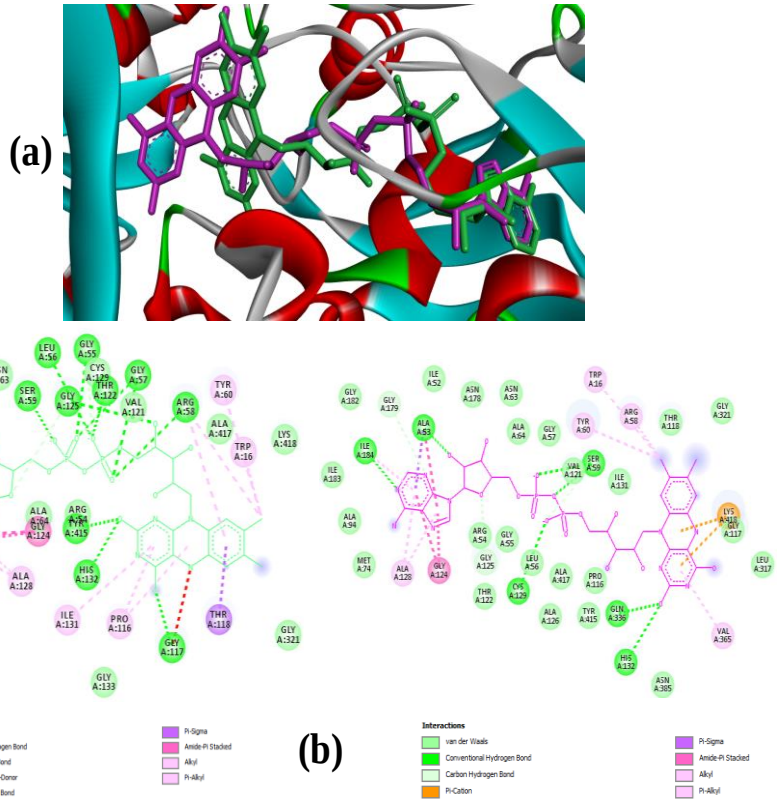

Figure-4: (a) 3D Binding modes of original Native ligand (Green color) and Redocked native ligand (Pink color) into the active site of target protein and (b) 2D interaction of original and redocked native ligand.

To validate the PASS prediction result molecular docking for anti-tubercular potential of the compounds **[3a-e]** was carried out on target protein PDB ID: 4FDO. Docked compounds **[3a-e], [ISO]** and **[PYR]** exhibited binding energies of -9.4 to -9.7 Kcal/mol, -6.0 Kcal/mol and -5.6 Kcal/mol respectively which is lower than the native ligand binding energy (-13.7 Kcal/mol) as tabulated in **table-8** and binding interactions are shown in **figure-5**.

Table-8: Molecular docking results of Native ligand and compounds

Code	**Docking energies (Kcal/mol)**
	Anti-tubercular
	PBD: 4FDO
Native Ligand	**-13.7**
3a	-9.6
3b	-9.7
3c	-9.4
3d	-9.5
3e	-9.6
ISO	-6.0
PYR	-5.6

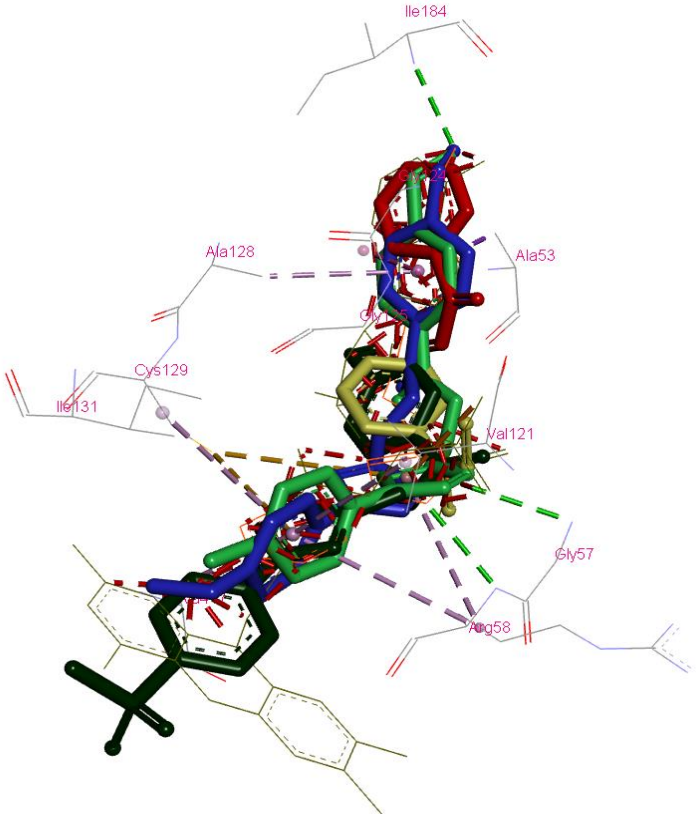

Figure-5: 3D Binding modes of [3a-e], [ISO] and [PYR] with active site of 4FDO target protein

CONCLUSION:

We have synthesised 1, 4-Disubstituted 1, 2, 3-Triazole 4-Formyl benzoate derivatives from commercially available starting materials with good to excellent yields. The structures of the compounds have been confirmed by multinuclear NMR spectroscopic technique. Additionally, PASS analysis showed that they may act as antimycobacterial agents and analysis of the ADME parameters showed good drug like properties and may act as poor oral drug candidate. Further, to validate PASS prediction and to know the binding mechanism molecular docking study of synthesized triazole derivatives were carried out and result showed that compounds possess good binding affinity towards the active site of DprE1 enzyme which provides a strong platform for new structure-based drug design. Thus, suggesting that compounds can be further optimized and developed as a lead molecule.

REFERENCES:

i. (a) D. B. Young.; M. D. Perkins.; K. Duncan.; C. E. Barry.; J. Clin. Invest.; 2008**, 118**, 1255; (b) L. Christian.; V. Andrew.; M. C. Raviglione.; Curr. Opin. Pulm. Med.; 2010, **16**, 186; (c) M. M. Sankar, J. Singh.; S. C. A. Diana.; S. Singh.; Tuberculosis.; 2013, **93**, 75.

ii. M. M. Singh.; Indian J.; Tuberc.; 2007, **54**, 1.

iii. S. Rani, K.; Raheja.; V. Luxami.; K. Paul.; Bioorg. Chem,; 2021, **113**, 105017.

iv. C. Menendez,; S. Gau.; C. Lherbet.; F. Rodriguez.; C. Inard.; M. R. Pasca.; and M. Baltas.; Eur. J. Med. Chem.; 2011, **46**, 5524.

v. C. Gill.; G. Jadhav.; M. Shaikh.; R. Kale.; A. Ghawalkar.; D. Nagargoje.; M. Shiradkar.; Bioor.; Med. Chem. Lett.; 2008, **18**, 6244.

vi. G. R. Labadie.; A. de la Iglesia,; H. R. Morbidoni.; Mol. Divers.; 2011, **15**, 1017.
vii. N. Boechat.; V. F. Ferreira.; S. B. Ferreira; M. L. G. Ferreir.; F. C. da Silv.; M. M. Bastos.; M. S. Costa.; M. C. S. Lourenço.; A. C. Pinto.; A. U. Krettl.i; A. C. Aguiar.; B. M. Teixeira.; N. V. da Silva.; P. R. C. Martins.; F. A. F. M. Bezerra.; A. L. S. Camil.; G. P. da Silva.; C. C. P. Costa, J. Med. Chem.; 2011, **54**, 5988.
viii. (a) M. H. Shaikh.; D. D. Subhedar.; L. Nawale.; D. Sarkar.; F. A. Kalam Khan.; J. N. Sangshetti.; B. B. Shingate.; Med. Chem. Commun.; 2015, **6**, 104-1116; (b) P. Shanmugavelan.; S. Nagarajan.; M. Sathishkumar.; A. Ponnuswamy.; P. Yogeeswari D. Sriram.; Bioorg. Med. Chem. Lett.; 2011, **21**, 7273; (c) K. I. Reddy.; K. Srihari.; J. Renuka.; K. S. Sree.; A. Chuppala.; V. U. Jeankumar.; J. P. Sridevi.; K. S. Babu.; P. Yogeeswari.; D. Sriram.; Bioorg. Med. Chem.; 2014, **22**, 6552.
ix. W. A. Rutala.; D .J. Weber.; New disinfection and sterilization methods, Emerg. Infect. Dis.; 2001, **7,** 348–353.
x. S. E. Walsh.; J. Y. Maillard.; A. D. Russell.; C. E. Catrenich.; D. L. Charbonneau.; R. G. Bartolo.; J. Hosp. Infect.; 2003, **55,** 98–107.
xi. S. A. Güngör.; M. Tümer.; M. Köse.; S. Erkan.; J. Mol. Struct.; 2020, **1206**, 127780.
xii. L. Zhu.; X. Xu.; F. Zheng.; Turkish J. Chem.; 2018, **42,** 75–85.
xiii. G. Krishnaswamy.; P. Raghuramshetty.; B. Roopa.; Salma banu.; H. J. Preritha.; B. S. Rajeshwar.; M. Ravikumar.; K. Pruthviraj.; D.B. Aruna kumar.; S. Sreenivasa.; Asian J. Chem.; 2020, **32**, 1857-1864.
xiv. A. Daina.; O. Michielin.; V. Zoete.; Sci. Rep.; 2017, **7,** 42717.
xv. (a) M. Fauzia.; S. Syed.; M. S. Zaman.; P. K. Nitin.; S. R. Vikrant.; M. Chaitanya.; M. Naveen.; A. K. Inshad.; M. S. Alam.; Eur. J. Med. Chem.; 2014, **76(** 274); (b) S. A. Stanley.; S. S. Grant.; T. Kawate.; N. Iwase.; M. Shimizu.; C. Wivagg.; M. Silvis.; E. Kazyanskaya.; J. Aquadro.; A. Golas.; M. Fitzgerald.; H. Dai.; L. Zhang.; D. T. Hung, ACS Chem. Biol.; 2012, **7,** 1377.
xvi. G. Riccardi,; M. R. Pasca.; L. R. Chiarelli.; G. Manina.; A. Mattevi.; C. Binda.; Appl. Microbiol. Biotechnol.; 2013, **87**, 8841.
xvii. O. Trott.; A. J. Olson.; J. Comp. Chem.; 2010, **31**, 455-461.
xviii. X. Creary.; A. Anderson.; C. Brophy.; F. Crowell.; Z. Funk.; J. Org. Chem.; 2012 **77**, 8756–8761.
xix. M. M. Rammah.; W. Gati.; H. Mtiraoui.; M. E. B. Rammah.; K. Ciamala.; M. Knorr.; Y. Rousselin.; M. M. Kubicki.; Molecules.; 2016, **21**, 307.

Received on November 27, 2022.